Proceedings of IMECE2006
2006 ASME International Mechanical Engineering Congress and Exposition
November 5-10, 2006, Chicago, Illinois, USA

IMECE2006-15055

SIMULATION OF PULVERIZED COAL INJECTION IN A BLAST FURNACE

Mingyan Gu, Zumao Chen, Naresh K Selvarasu, D. (Frank) Huang*, Pinakin Chaubal*, and Chenn Q. Zhou

Department of Mechanical Engineering, Purdue University Calumet, Hammond, IN 46321
*** USA R&D Center, Mittal Steel Company, East Chicago, Indiana 46312, U.S.A**

ABSTRACT

A three-dimensional multiphase CFD model using an Eulerian approach is developed to simulate the process of pulverized coal injection into a blast furnace. The model provides the detailed fields of fluid flow velocity, temperatures, and compositions, as well as coal mass distributions during the devolatilization and combustion of the coal. This paper focuses on coal devolatilization and combustion in the space before entering the raceway of the blast furnace. Parametric studies have been conducted to investigate the effect of coal properties and injection operations.

Keywords: Blast Furnace, CFD, Devolatilization, Combustion, Ironmaking, PCI

INTRODUCTION

Blast furnace ironmaking is a major process for hot metal production. In order to reduce the cost of the hot metal production, since 1990, coal has become the injectant choice because of its relative abundance and low cost.

Pulverized coal is injected into the tuyere with the blast of high temperature and velocity. The extent of burnout of pulverized coal within the tuyere and within the raceway determines the temperature in the raceway and the permeability of raceway boundary. If coal particles in the combustion zones undergo incomplete combustion, the unburned or residual char will accumulate in the blast furnace. The char will be gasified by its reactions with the slag and/or the carbon dioxide in the gas, and the direct reduction of FeO. If the accumulation rate of the char in the furnace is larger than the reduction (or gasification) rate, the movement of hot blast will be retarded and high blast pressure issues may occur [1].

Abundant fundamental studies have been accomplished for understanding the injected coal combustion thermodynamically and kinetically. Based on the achieved thermodynamics and kinetics of coal and coke combustions, mathematical modeling for detailed numerical simulations is helpful to aid in evaluating and predicting the optimum conditions for coal injection [2-9]. Earlier modeling efforts assumed one-dimensional plug flow for the tuyere and the raceway [4], and thus could not predict correctly the commencement of coal devolatilization and combustion of released volatiles. Two-dimensional models consisting of a coal combustion model and a coke combustion model in the raceway were later developed, turbulent features of the gas phase were either ignored [7] or simulated with a modified turbulence model [8]. However, two-dimensional models can only be used in simple geometry conditions. For complex geometries such as different lance arrangements used to enhance injected coal combustion in the tuyere-raceway system, a more practical and realistic three-dimensional model is required. More recently, commercial software was utilized to simulate coal devolatilization and combustion in a combustion chamber (ANSYS-CFX4) [5] or in a tuyere-raceway system with an assumed raceway shape (Fluent) [9]. In these simulations, the particle phase was treated as a dispersed phase using a Lagrangian method and a stochastic model was used to calculate particle turbulent dispersion. This method can only be used to simulate pulverized coal injection with a lower solid volume fraction, since this approach often ignores particle-particle interactions and the effect of particle volume fraction on the gas phase [10]. Recently, a multi-phase model for turbulent reacting flows was reported [6], in which both the gas phase and the particle phase were treated as two interpenetrating continua in an Eulerian frame of reference.

In this paper, a three-dimensional (3-D) multi-phase computational fluid dynamics (CFD) model using an Eulerian approach is developed to simulate pulverized coal flow, devolatilization as well as combustion in the tuyere. Effects of particle diameters are investigated.

MATHEMATICAL MODEL

Governing equations

Gas-phase continuity, momentum, species mass fraction and energy equations as well as the equations of the turbulent kinetic energy and its dissipation rate at steady state can be written in the following generalized form

$$\text{div}\ (\rho \mathrm{u}\phi) = \text{div}\,(\Gamma_\phi\ \text{grad}\ \phi) + S_\phi + S_{P\phi} \qquad (1)$$

where ϕ is the independent variable, Γ_ϕ is the effective transport coefficient, S_ϕ and $S_{P\phi}$ are source terms of the gas phase itself and the source term due to the presence of particles, respectively. Detailed information on these parameters for each equation can be found elsewhere [6, 11].

Coal particle phase governing equations describing its mass, momentum and energy for steady state flows can be written in the following generalized form

$$\text{div}\ (\alpha \mathrm{u}_\mathrm{k}\phi_\mathrm{k}) = \text{div}\,(\Gamma_\mathrm{k}\ \text{grad}\,\beta\phi_\mathrm{k}) + S_\mathrm{pk} \qquad (2)$$

where k indicates the k-group particle, ϕ_k is the independent variable, Γ_k is the effective transport coefficient, S_{PK} is the source term including both the particle phase itself and the source term due to the interaction with the gas phase. Definition of these variables for each equation can be found in reference [12].

Turbulence model

The standard k-ε model is used for modeling the gas phase turbulence. The source terms due to the interaction between the gas phase and the particle phase are G_P and G_R.

$$G_p = \sum_k \frac{2\rho_k}{\tau_{rk}}\left(C_p^k\sqrt{kk_k} - k\right) \qquad (3)$$

$$G_R = -k\sum_k n_k m_k \qquad (4)$$

where k_k is the k-group particle phase turbulent kinetic energy. When the gas phase turbulent kinetic energy is larger than that of the particle phase, this term will cause the reduction of gas phase turbulent kinetic energy. On the other hand, when the particle phase turbulent kinetic energy is larger than that of the gas phase, it gives rise to the production of gas phase turbulent kinetic energy. Therefore, this term represents the balance mechanism between the gas phase turbulence and the particle phase turbulence. Another source term G_R is due to the mass change in the particle phase.

Drag force between the particle and the gas phase

The particle phase exchanges momentum with the gas phase through the drag force. The exchange coefficient can be expressed as

$$\beta_k = \frac{3}{4}C_D\frac{|\mathrm{u}-\mathrm{u}_k|(1-\varepsilon_k)^2\rho\varepsilon_k}{d_k}f(\varepsilon_k) \qquad (5)$$

In the above equation, $f(\varepsilon_k)$ accounts for the effect of the presence of other particles and is a correction to the Stokes law for free fall of a single particle. The following equation is used in this work [13, 14]

$$f(\varepsilon_k) = (1-\varepsilon_k)^{-3.8} \qquad (6)$$

(1)

Gas combustion model

The eddy breakup (EBU) turbulent combustion model is used to quantify the effect of turbulence on the combustion rates of volatiles, carbon monoxide and hydrogen. The reaction rate is determined as: $\mathrm{W_s} = \min(\mathrm{W_{s,EBU}}, \mathrm{W_{s,Arr}})$

where

$$W_{s,Arr} = B_s\rho^2 Y_F Y_{ox}\exp(-\frac{E_s}{RT}) \qquad (7)$$

$$W_{s,EBU} = C_R\rho\frac{k}{\varepsilon}\min(Y_F, \frac{Y_{ox}}{\beta}) \qquad (8)$$

Heat transfer between coal particles and the gas

Heat transfer between a single reacting particle and the gas phase can be calculated as [12]:

$$Q_\mathrm{k} = \pi d_\mathrm{k} Nu_\mathrm{k}\lambda_\mathrm{s}(T-T_\mathrm{k})\frac{B_\mathrm{k}}{\exp(B_\mathrm{k})-1} \qquad (9)$$

$$B_\mathrm{k} = -\frac{\dot{m}_\mathrm{k}\,C_\mathrm{ps}}{\pi d_\mathrm{k} Nu_\mathrm{k}\lambda_s} \qquad (10)$$

$$Nu_k = 2 + 0.5\,\mathrm{Re}_k^{0.5} \qquad (11)$$

where the so-called 1/3 Law is used to calculate the thermal conductivity λ_s and C_ps around the coal particles.

Moisture evaporation rate

Assuming that the moisture in a coal particle diffuses to the surface of coal particle to form a liquid film and this film is treated as a surface layer of a water droplet with the same diameter, the moisture evaporation rate is calculated by a diffusion model [12].

$$\dot{m}_{wk} = \begin{cases} -\pi d_\mathrm{k} Nu_\mathrm{k} D_\mathrm{s}\rho_\mathrm{s}\ln\left(1+\dfrac{Y_{\mathrm{H_2O}s}-Y_{\mathrm{H_2O}g}}{1-Y_{H_2O,s}}\right) & T_\mathrm{k} < T_\mathrm{b} \\ -\pi d_\mathrm{k} Nu_\mathrm{k}\dfrac{\lambda_\mathrm{s}}{C_\mathrm{ps}}\ln\left(1+\dfrac{C_\mathrm{ps}(T-T_\mathrm{k})}{1-L_\mathrm{w}}\right) & T_\mathrm{k} \geq T_\mathrm{b} \end{cases} \qquad (12)$$

$$Y_{H_2O,s} = B_w\exp(-E_w / RT_k) \qquad (13)$$

where $Y_{H_2O,s}$ is the mass fraction of vapor at the surface of the coal particles.

DAF coal devolatilization rate

The coal devolatilization rate is proportional to the mass of the DAF (dry and ash free) coal. The coal devolatilization is modeled by two simultaneous, competing, first-order, irreversible reactions [15].

$$\text{DAF coal} \begin{cases} (1-\alpha_1)\,\text{Ch}_1 + \alpha_1 V_1 & (\text{Reaction } 1) \\ (1-\alpha_2)\,\text{Ch}_2 + \alpha_2 V_2 & (\text{Reaction } 2) \end{cases}$$

The volatile release rate is given by

$$\dot{m}_{vk} = -\alpha_1 m_{dk} B_{v1} \exp\left(-\frac{E_{v1}}{RT_k}\right) - \alpha_2 m_{dk} B_{v2} \exp\left(-\frac{E_{v2}}{RT_k}\right) \quad (14)$$

where α_1 is obtained from the volatile matter percentage in the proximate analysis of coal and α_2 is equal to $2\alpha_1$.

The daf coal mass reduction rate can be obtained by:

$$\dot{m}_{dk} = -m_{dk} B_{v1} \exp\left(-\frac{E_{v1}}{RT_k}\right) - m_{dk} B_{v2} \exp\left(-\frac{E_{v2}}{RT_k}\right) \quad (15)$$

Once the volatile matters are released in the gas phase, they undergo homogeneous combustion. In this work, it is assumed that the volatile consists of hydrocarbons and carbon monoxide only. The following three gaseous reactions are considered [16].

$$C_dH_b + \frac{d}{2}O_2 = d\,CO + \frac{b}{2}H_2 \quad (16)$$

$$C_dH_b + (d+\frac{b}{4})O_2 = d\,CO_2 + \frac{b}{2}H_2O \quad (17)$$

$$C_dH_b + \frac{2d+b}{4}O_2 = d\,CO + \frac{b}{2}H_2O \quad (18)$$

$$2CO + O_2 \rightarrow 2CO_2 \quad (19)$$

$$2H_2 + O_2 \rightarrow 2H_2O \quad (20)$$

Char reaction rate

The heterogeneous char reaction rate is assumed to be of first- order with respect to oxygen, carbon dioxide and water vapor concentrations.

$$C + O_2 \rightarrow CO_2 \quad (21)$$

$$2C + O_2 \rightarrow 2CO \quad (22)$$

$$C + CO_2 \rightarrow 2CO \quad (23)$$

$$C + H_2O \rightarrow CO + H_2 \quad (24)$$

The char reaction rates for the surface reactions (21) to (24) given in terms of the gas consumption rates can be written as:

$$\dot{m}_{ck,A} = -\pi d_k^2 \rho_s Y_{O_2,s} B_A \exp\left(-\frac{E_A}{RT_k}\right) \quad (25)$$

$$\dot{m}_{ck,B} = -\pi d_k^2 \rho_s Y_{O_2,s} B_B \exp\left(-\frac{E_B}{RT_k}\right) \quad (26)$$

$$\dot{m}_{ck,C} = -\pi d_k^2 \rho_s Y_{CO_2,s} B_C \exp\left(-\frac{E_C}{RT_k}\right) \quad (27)$$

$$\dot{m}_{ck,D} = -\pi d_k^2 \rho_s Y_{H_2O,s} B_D \exp\left(-\frac{E_D}{RT_k}\right) \quad (28)$$

Table 1 Reaction kinetic constants [6]

Chemical/ physical process	B	Unit	E (J/mol)
Moisture evaporation	8.32×10^5		4.228×10^4
Devolatilization (Reaction 1)	3.7×10^5	s^{-1}	7.366×10^4
Devolatilization (Reaction 2)	1.46×10^{13}	s^{-1}	2.511×10^5
Char reaction (25)	1.225×10^3	ms^{-1}	9.977×10^4
Char reaction (26)	1.813×10^3	ms^{-1}	1.089×10^5
Char reaction (27, 28)	7.351×10^3	ms^{-1}	1.380×10^5

The reaction kinetic constants used in this paper are given in Table 1. Radiative heat transfer is calculated by the discrete-ordinates model [17].

The SIMPLE algorithm [18] is used to solve the gas phase equations; a similar procedure is used for the particle phase, but without the p-v corrections. A Tri-diagonal matrix algorithm (TDMA) with under-relaxation factors is applied to solve the finite difference equations. The convection-diffusion flux is evaluated using an upwind scheme.

SIMULATION CONDITIONS

Figure 1 shows the geometry. The injection lance is introduced into the tuyere upstream of the tuyere at an inclination of 4˚ to the tuyere central line and to the right with an angle of 10.8˚ according to a real PCI system. The lance has an inner diameter of 0.019m. The calculation domain is $0.196\text{m}\times0.196\text{m}\times0.58\text{m}$, the mesh system of $60\times60\times60$ is adopted based on rectangular coordinate

system. The tuyere inner zone is gradually narrowed from a diameter of 166mm to 150mm in a distance 0.24m. The inlet conditions used are summarized in Table 2, the blast is oxygen-enriched with 8 m^3 oxygen/100 m^3 air; the carrier gas is N_2 with a solid volume fraction of 10%. Adiabatic boundary conditions are imposed at the walls. Coal proximate and ultimate analyses are given in Table 3 and 4, respectively.

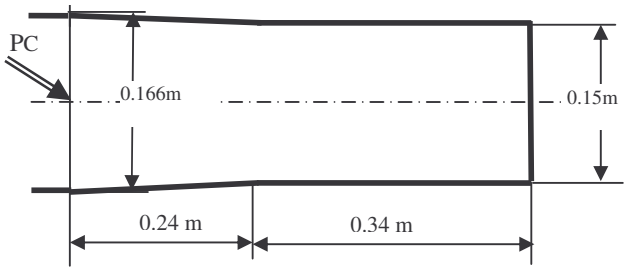

Fig. 1 Tuyere pipe inner size

Table 2 Inlet parameters

Blast	
Flow rate (kg/s)	3.44
Temperature (K)	1493
Pressure at the tuyere (Pa)	4.613E+5
Coal particle	
Flow rate (kg/s)	0.38
Average diameter (μm)	30, 60, 90
Carrier gas (N_2)	
Flow rate (kg/s)	0.014
Temperature (K)	360

Table 3 Coal proximate analysis (wt %, ad)

Fixed carbon	Volatile matter	Moisture	Ash
56.49	34.32	3.6	5.59

Table 4 Coal ultimate analysis (wt, %)

C	H	O	N	S	Ash
81.70	5.00	4.90	1.73	0.87	5.80

RESULTS AND DISCUSSION

In this section, simulation results for a particle diameter of 60 μm will be discussed in detail. The effect of particle diameters on the devolatilization and coal burnout will also be discussed.

Figure 2 shows the gas temperature distribution and Fig.3 shows gas velocity distribution. The inclined lance and coal plume cause the flow field to be asymmetric, and the higher temperature occurs in the lower half region. This can be seen more clearly in Figs. 4-7. The oxygen concentration in the coal plume region is low due to combustion of volatile and char combustion. An annular region of high temperature is formed at the plume surface, where higher oxygen content causes rapid reaction of volatile matters and release of heat.

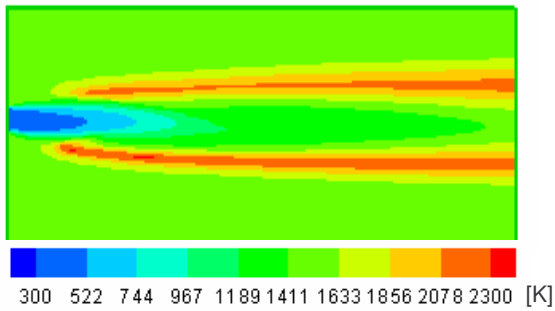

Fig. 2 Gas temperature distribution in a plane across tuyere centerline (coal particle size 60 μm)

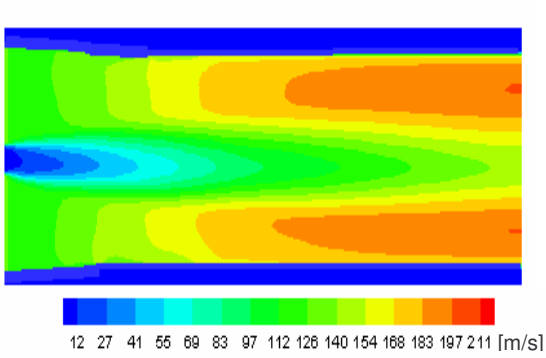

Fig. 3 Gas velocity distribution in a plane across tuyere centerline (coal particle size 60 μm)

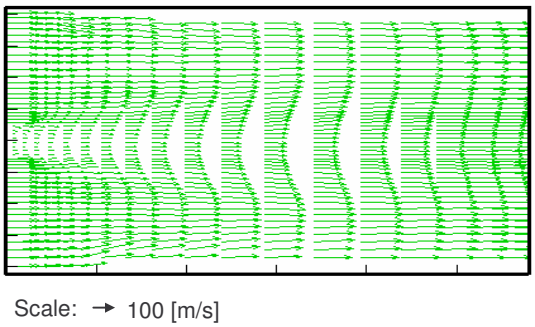

Fig.4 Gas velocity vectors

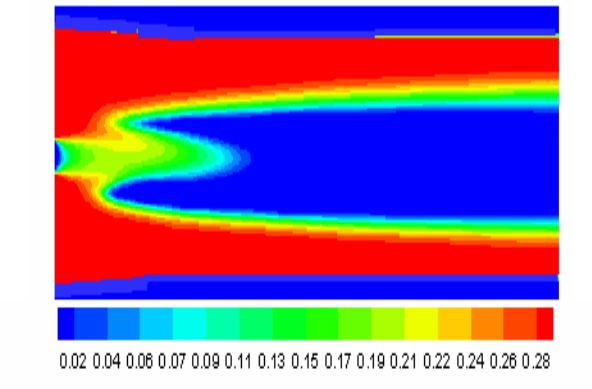

Fig. 5 Oxygen mass fraction distribution in a plane across tuyere centerline (coal particle size 60 μm)

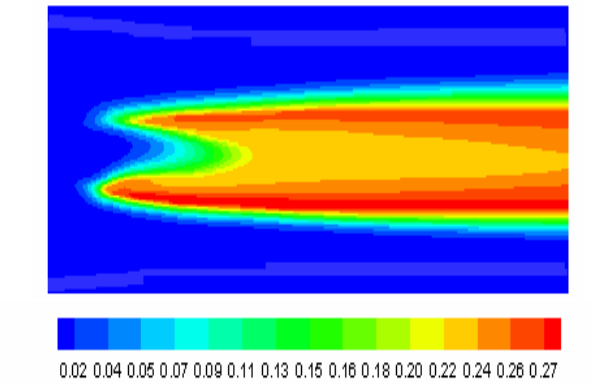

Fig. 6 CO mass fraction distribution in a plane across tuyere centerline (coal particle size 60 μm)

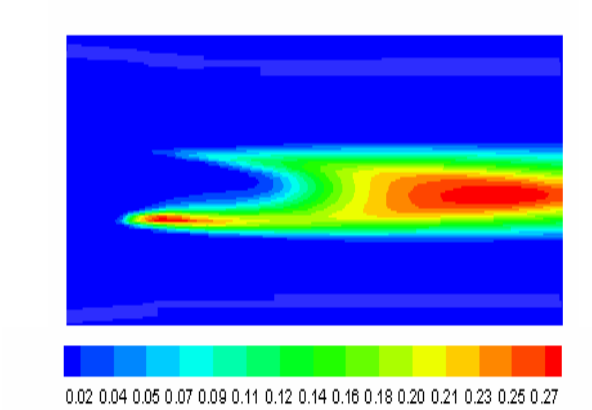

Fig. 7 Volatile matter fraction distribution in a plane across tuyere centerline (coal particle size 60 μm)

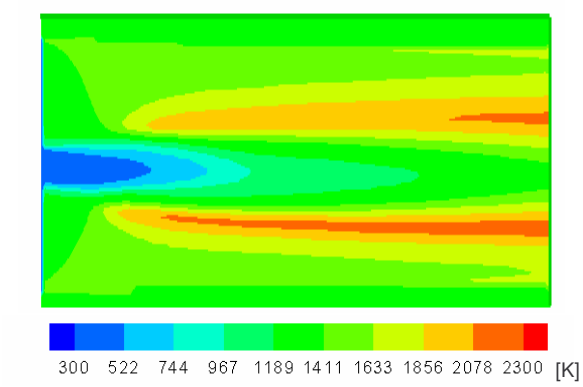

Fig. 8 Particle temperature distribution in a plane across tuyere centerline (coal particle size 60 μm)

Figure 8 shows the particle temperature distribution. Compared with Fig. 2, it can be seen that the particle temperature has a similar distribution and is a little bit lower than the gas temperature.

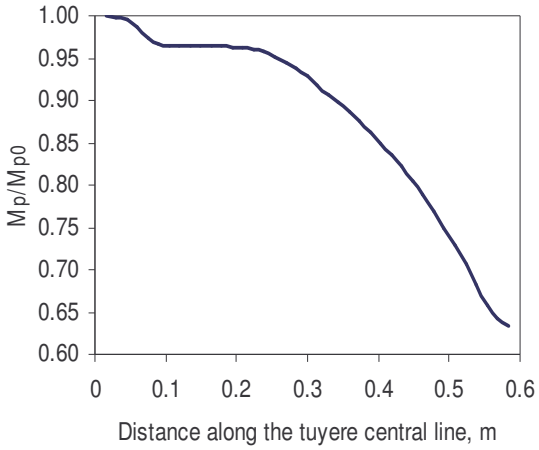

Fig. 9 The relative coal mass distribution along the tuyere central line.

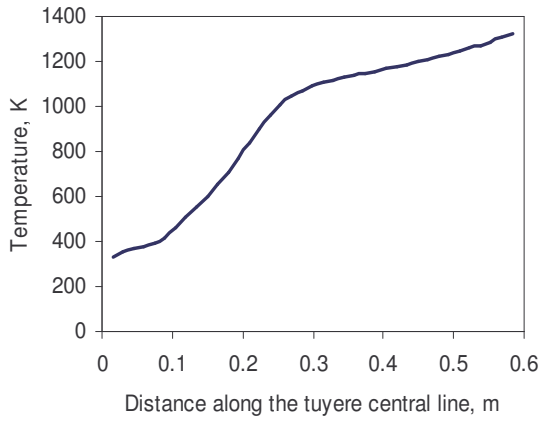

Fig. 10 Coal particle temperature distribution along the tuyere central line.

Figures 9 and 10 show the pulverized coal mass and temperature distributions along the tuyere center line, respectively. M_{p0} is the coal particle original weight and M_p is the coal particle weight. When the coal is injected into the tuyere, the particle is heated up by the high temperature blast, so the moisture vaporizes rapidly. After particles are heated in a distance about 0.2m, rapid coal devolatilization occurs; when the particles move toward the exit of tuyere, the total volatile matter is nearly completely released and the slow char combustion commences, so the mass reduction rate slows down.

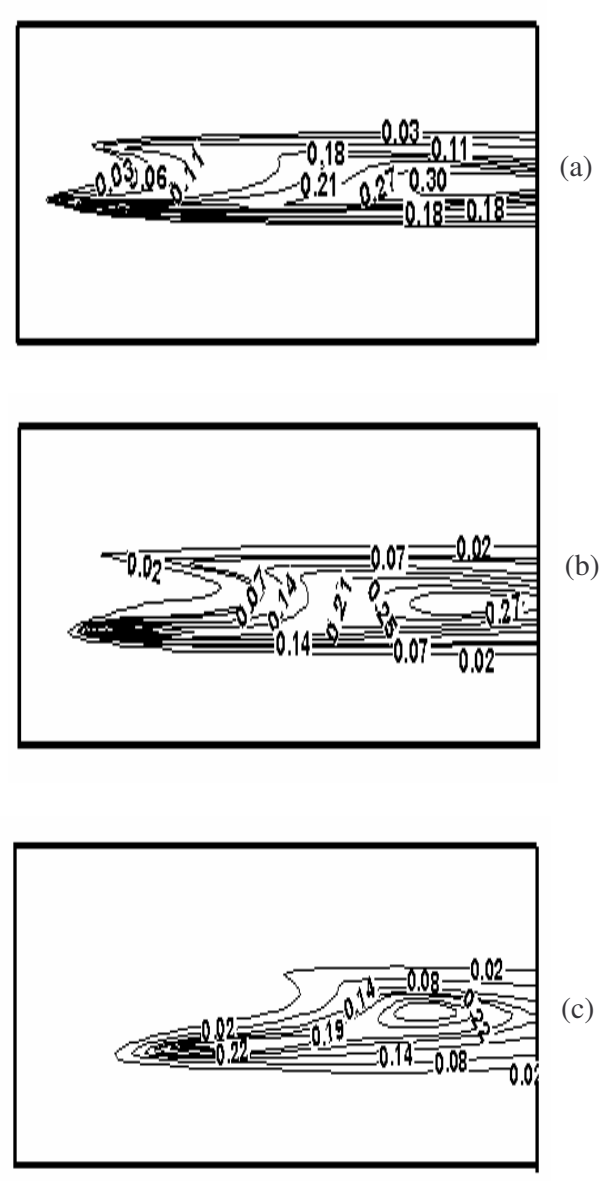

Fig. 11 Volatile matter mass fraction distribution
(a) dp =30 μm (b) dp=60 μm (c) dp=90 μm

Figure 11 shows the volatile matter concentration distribution for three particle diameters of 30 μm, 60 μm and 90 μm, respectively. For the small particles, the heating rate is highest, so the volatile matters start to release at the shortest distance from the injection location. The figure also shows that, for the particle diameter of 90 μm, the volatile matter distribution exhibits more asymmetrically because of the higher particle inertia. Due to the short residence time inside the tuyere and the lower oxygen concentration in the coal plume region, the combustion of volatile matter released from coal is not complete and the concentration of volatile matter at the exit of tuyere is still high for all the three cases.

The burnout represents the total weight loss of the coal due to moisture evaporation, volatile release and char combustion. Here the burnout is defined as:

$$B = m_e / m_0 \times 100\% \qquad (29)$$

Where m_0 is the original coal weight and m_e is the weight-loss of coal.

Figure 12 represents the burnout at the exit of the tuyere. It can be seen clearly that the particle sizes have a great effect on the burnout; the particles with a smaller diameter have a higher burnout than the larger one.

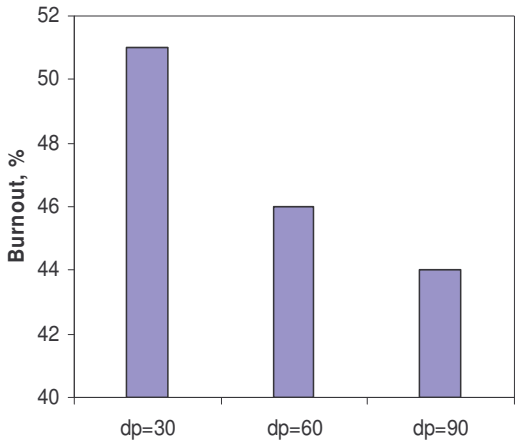

Fig. 12 Burnout of pulverized coal

SUMMARY

A three-dimensional mathematical model has been developed to simulate coal devolatilization and combustion inside the tuyere. The simulated results show that volatile matter releases rapidly from the pulverized coal inside the tuyere; partially volatile matter burns before exiting the tuyere. The pulverized coal size has an important effect on the coal burnout. The bigger the coal particle, the lower the burn-out rate. The lance inclined angle and the pulverized coal affect the flow field inside the tuyere. For the same lance angle, the greater the particles diameter, the more asymmetric the flow field.

ACKNOWLEDGEMENT

The authors are grateful to the financial support of American Iron and Steel Institute (AISI) (Award No. TRP9945).

NOMENCLATURE

C_D	drag coefficient between gas and one droplet
d_p	particle diameter, m
D	diffusivity, m^2/s
E	activation energy, J/mol
k	gas phase turbulent kinetic energy, m^2/s^2
$\dot{m}$	particle mass change, kg/m^3 bed·s
n	particle phase number density, 1/m3
P	pressure, Pa
S	gas-phase source term per unit volume, kg/m^3
u	velocity, m/s
W	reaction rate, kg/s
Y	species mass fraction

Greek symbols

ε	dissipation rate of gas phase turbulent kinetic energy, m^2/s^3
μ	viscosity, kg/m·s
ϕ	independent variable
ρ	density, kg/m^3
Γ	effective transport coefficient

Subscripts

g	gas phase
k	k-group particle phase
p	particle

REFERENCES

[1] Kuniyoshi Ishii,Advanced pulverized coal injection technology and blast furnace operation, Pergamon Press, Elsevier science Ltd, UK, 2000.

[2] Shan-Wen Du, Wei-Hsin Chen, 2006, "Numerical prediction and practical improvement of pulverized coal combustion in blast furnace", International communications in Heat and Mass Transfer, 33, 327-334.

[3] Ching-Wen Chen, 2005, "Numerical analysis for the multi-phase flow of pulverized coal injection inside balst furnace tuyere", Applied Mathematical Modelling, 29, 871-884.

[4] A.S. Jamaluddin, T.F. Wall and J.S. Truelove, 1986, "Mathematical modeling of combustion in blast furnace raceways, including injection of pulverized coal", Ironmaking and Steelmaking, 13, 91-99.

[5] B. Guo, P. Zulli, H. Rogers, J.G. Mathieson and A. Yu, 2005, "Three-dimensional simulation of flow and combustion for pulverized coal injection", ISIJ. 9, 1272-1281.

[6] Guo Y. C., Chan C. K. and Lau K. S., 2003, "Numerical studies of pulverized coal combustion in a tubular coal combustor with slanted oxygen jet", Fuel, 82, 893-907.

[7] H. Nogami, T. Miura and T. Furukawa, 1992, "Simulation of transport phenomena around raceway zone in the lower part of blast furnace", Tetsu-to-Hagane, 78, 1222 -1229.

[8] K. Takeda and F. C. Lock wood, 1997, "Integrated mathematical model of pulverized coal combustion in a blast furnace", ISIJ International, 37, 432-440.

[9] M. Picard, 2001, "Pulverized coal combustion in the blast furnace raceway, using a 3D numerical simulation", Proceedings of the 2001 Ironmaking Conference.

[10] Fluent. Inc. 2005, " Overview and limitation of the doscrete phase models", 23.1.

[11] L. X. Zhou, L. Li, R.X. Li, J. Zhang, 2002," Simulation of 3-D gas-particel flows and coal combustion in a tangentially fired furnace using a two-fluid-trajectory model", Power Technology, 125, 226-233.

[12] Zhou L.X., Theory and numerical modeling of turbulent gas-particle flows and combustion, Boca Raton, Science Press/CRC Press Inc, 1993.

[13] Gibilaro L. G., Di Felice R., Waldram S.P. and Foscolo P.U., 1985, "Generalised friction factor and drag coefficient correlations for fluid-particle interactions". Chem. Eng. Sci., 40, 1817.

[14] Chen Z., Gibilaro L.G. and Foscolo P.U., 1999, "Two-dimensional voidage waves in fluidized beds", Ind. Eng. Chem. Res., 38, 610-620.

[15] Ubhayakar S.K., Stickler D.B., von Rosenberg C.W. and Gannon R.E., 16th Symp.(Int.) Comb., Combustion Inst., Pittsburgh, 1977, 427.

[16] Kalyan Annamalai and William Ryan, 1993, "Interactive processes in gasifigation and combusiton- II. Isolated carbon, coal and porous char particles", Prog. Energy Combust. Sci, 19, 383-446.

[17] Fiveland W. A., 1991, "The selection of discrete ordinate quadrature sets for anisotropic scattering", HTD, 160, Fundamentals of Radiation Heat Transfer, ASME, New York, 89-96.

[18] Patankar S. V., Numerical heat transfer and fluid flow, Hemisphere Publishing Corporation, 1980.